On-Line Supplementary Information

Far-Field Photostable Optical Nanoscopy (PHOTON) for Real-Time Super-Resolution Single-Molecular Imaging of Signaling Pathways of Single Live Cells

Tao Huang, Lauren M. Browning and Xiao-Hong Nancy Xu*

Department of Chemistry and Biochemistry, Old Dominion University, Norfolk, VA 23529

* To whom correspondence should be addressed: Email: xhxu@odu.edu; www.odu.edu/sci/xu/xu.htm; Tel/fax: (757) 683-5698

The on-line supplementary information includes:

(A) Table S1: Summary of dependence of apoptosis upon binding and endocytosis of single L-R complexes;

(B) Nine Supporting Figures and Figure Caption

Fig. S1: NMR characterization of functional groups attached on the surface of Ag NPs.

Fig. S2: Cross-sections of self-assembly monolayer of MUA and MCH, and citrate molecules attached on the surface of NPs show footprint areas of the attached molecules.

Fig. S3: Characterization of binding affinity and dynamic ranges of SMNOBS.

Fig. S4: Mapping of number (four) and centroids (precise locations) of single SMNOBS bound with TNFR1 molecules on single live cells using deconvolution and PSF.

Fig. S5: Nanometer-Resolution imaging of single SMNOBS bound with single TNFR1 molecules on single live cells using PHOTON.

Fig. S6: Mapping of number (one) and centroids (precise locations) of single SMNOBS bound with TNFR1 molecules on single live cells using deconvolution and PSF.

Fig. S7: Nanometer-Resolution imaging of single SMNOBS bound with single TNFR1 molecules on single live cells using PHOTON.

Fig. S8: Blank control experiments for the cells incubated with the cell culture medium alone.

Fig. S9: Control experiment for the cells incubated with AgMMUA NPs in the medium.

(C) Two Videos

Video S1: Real-time super-resolution SM imaging of dynamic cascades (SMNOBS bound with TNFR1, formation of its clusters, their endocytosis, and cellular apoptosis) of TNFα-induced apoptotic signaling pathways of single live cells using PHOTON.

Video S2: An example of real-time tracking the diffusion trajectory of single L-R complexes on single live cells over time.

A. Table S1: Summary of Dependence of Apoptosis on Binding and Endocytosis Dynamics of Single Ligand-Receptor Complexes on Single Live Cells

Group	Cell[a]	t_b [b] (min)	t_e [c] (min)	t_a [d] (min)	Max. # of Surface L-R [e]	# of Surface L-R [f]	# of Internalized L-R [g]
A	1	9	60	282	515	435	372
	2	12	81	300	455	383	276
B	3	12	81	321	308	291	180
C	4	12	81	342	486	357	216
	5	12	102	360	515	396	276
	6	15	81	342	633	453	525
D	7	21	102	360	316	273	180
	8	21	102	360	293	282	264
	9	21	102	360	365	298	132
	10	21	102	381	285	255	192
	11	21	102	381	238	214	168
	12	21	102	381	418	246	228
E	13	24	141	381	375	288	192
	14	24	141	381	327	265	216
	15	27	141	402	216	198	156
	16	27	141	402	296	276	180
F	17	30	162	462	155	141	96
	18	30	162	480	168	147	108
G	19	36	162	540	134	110	60
	20	36	162	582	125	98	72
	21	39	162	600	130	85	60
	22	39	162	621	117	81	72
	23	39	162	642	93	78	84
H	24	42	201	702	84	72	36
	25	42	201	702	112	73	72
	26	42	201	720	72	68	60

[a]: cells marked by a number
[b]: initial binding time of single TNFα (L) molecules (SMNOBS) with TNFR1 (R) on single live cells
[c]: initial endocytosis time of single L-R complexes into single live cells
[d]: initial apoptosis time of single live cells
[e]: maximum number of single L-R complexes on single live cells
[f]: number of single L-R complexes on single live cells at the initial apoptosis time (t_a)
[g]: number of internalized single L-R complexes of single live cells at the initial apoptosis time (t_a)

B. Supplementary Figures and Figure Captions

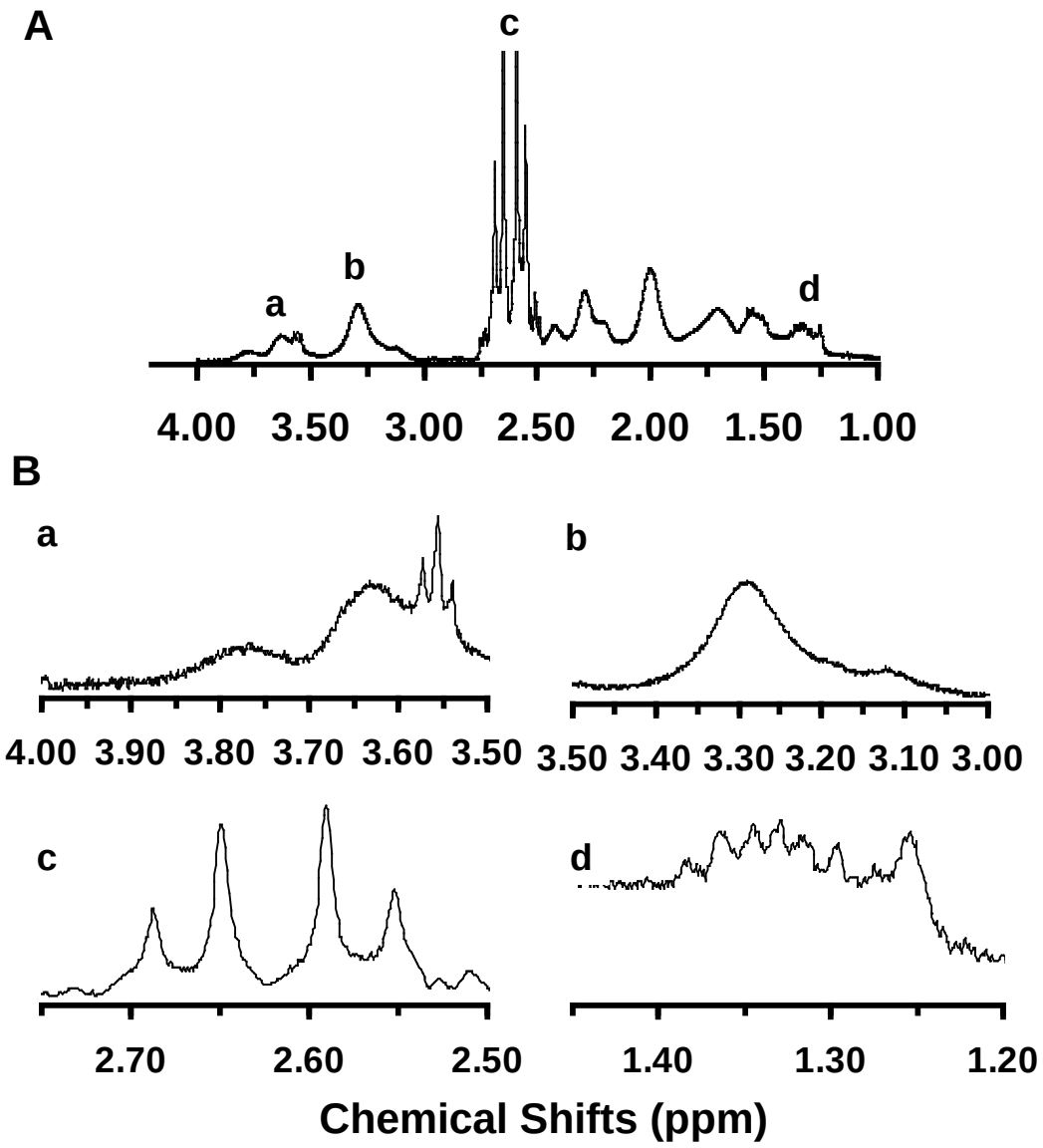

Fig. S1: NMR characterization of functional groups (citrate, MUA, MCH, PVP) attached on the surface of Ag NPs. **(A)** NMR spectra of AgMMUA NPs, and **(B)** zoom-in peaks of NMR spectra in (A) show: (a) δ = 3.55 ppm, integration = 1.68 (**2H** in -(CH_2)-OH of MCH); (b) δ = 3.28 ppm, integration = 4.15 (**2H** from PVP ring); (c) δ = 2.62 ppm, integration = 25.52 (-C**H_2**- next to thiol from both MUA and MCH and **4H** from citrate); (d) δ = 1.20-1.45 ppm, integration = 5.46 (**12H** from –**$(CH_2)_6$**-CH_2COOH of MUA and **4H** from –**$(CH_2)_2$**-CH_2OH of MCH). Molar ratio of citrate : MCH : MUA : PVP = 34 : 5 : 1 : 0.02, shows a single carboxyl group per NP, as determined by a close-packing model (Fig S2).

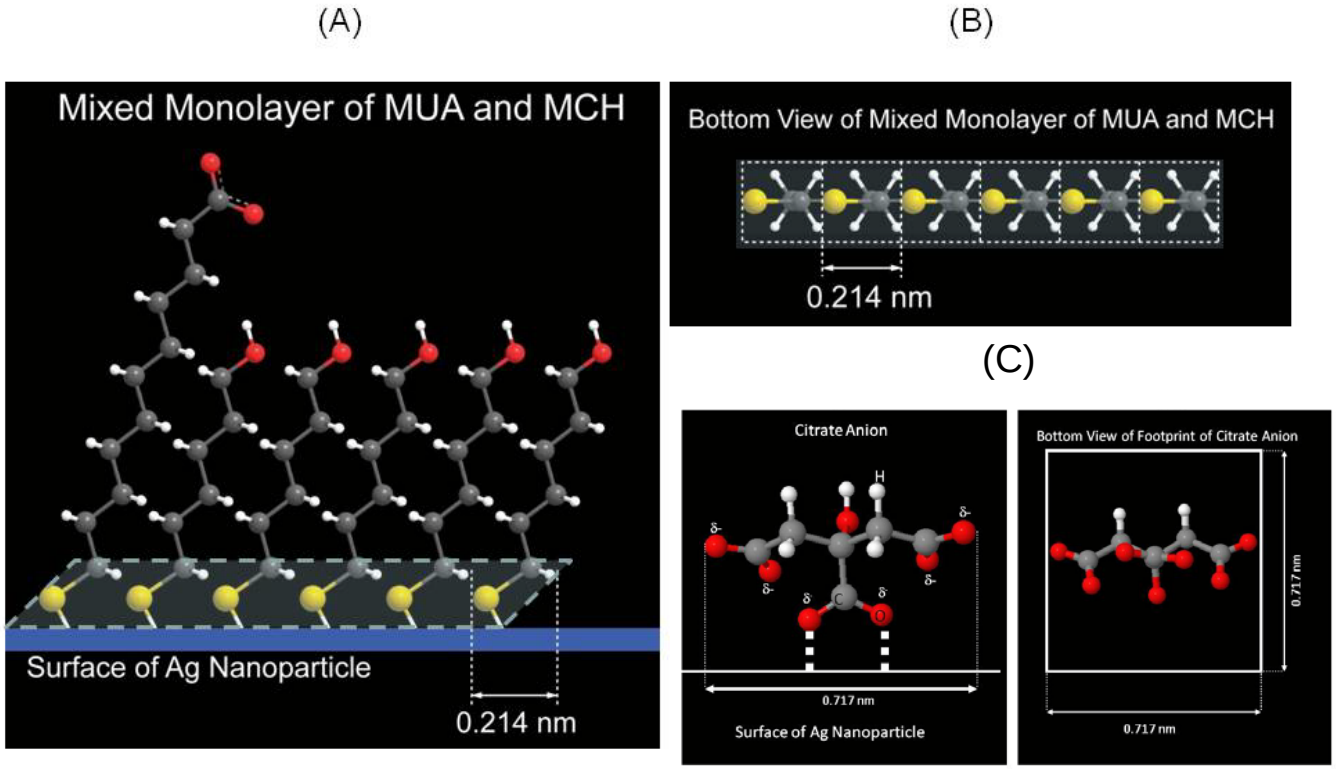

Fig. S2: Close-packing model of self-assembly monolayer of mixed MUA and MCH molecules and adsorbed citrate anion on the surface of Ag NPs shows the footprint area of individual molecule of MUA and MCH at 0.0458 nm^2 (0.214 nm x 0.214 nm) and citrate molecule at 0.514 nm^2 (0.717 nm x 0.717 nm): **(A)** side-view and **(B)** bottom-view of the close-packing monolayer of mixed MUA and MCH, and **(C)** side-view and bottom-view of the adsorbed citrate molecules on the surface of Ag NPs.

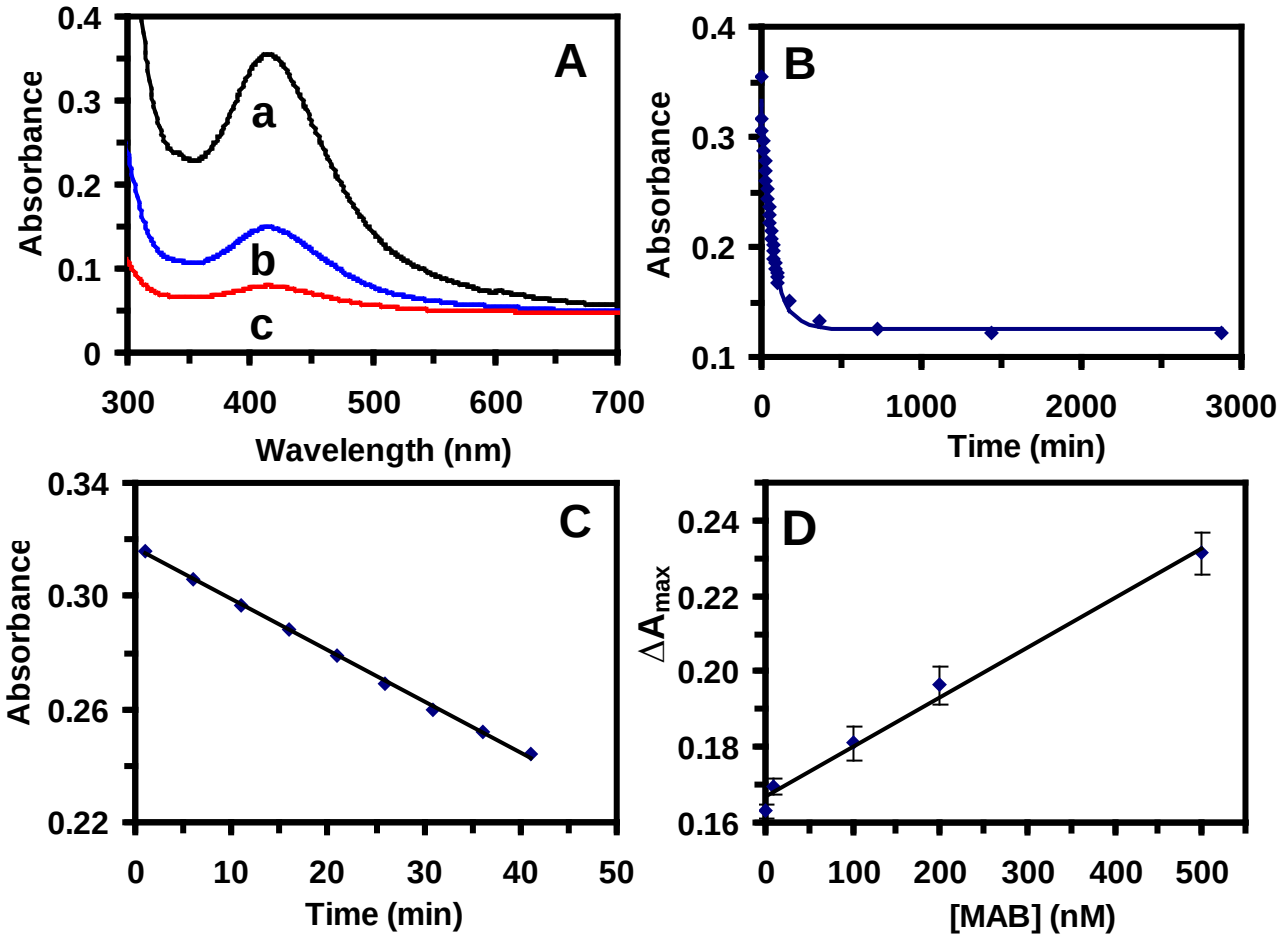

Fig. S3: Characterization of binding affinity, binding kinetics and dynamic range of SMNOBS (AgMMUA-TNFα NPs) with monoclonal antibody of TNFα (MAB): **(A)** UV-vis absorption spectra of AgMMUA-TNFα NPs (50 nM) incubated with MAB (500 nM) in PBS buffer (10 mM, pH 7.4) at (a) 0, (b) 21 min, and (c) 24 h, show an unchanged absorption peak wavelength (λ_{max}) at 414 ± 2 nm and a decrease in absorbance over time. **(B)** Plot of the peak absorbance subtracted by baseline in (A) versus the incubation time, illustrates the exponential decay ($A = 0.13 + 0.21e^{-0.014t}$ with the linear regression (R^2) = 0.99). **(C)** Zoom-in plot of (B) during 0 to 40 min shows high linearity with a slop of -1.8×10^{-3} min^{-1} and R^2 of 0.99. **(D)** Plot of the maximum decreased absorbance (ΔA_{max} = background subtracted peak absorbance of SMNOBS prior to their incubation with MAB - background subtracted peak absorbance of SMNOBS at the binding equilibrium with MAB) versus concentrations of MAB (calibration curve of SMNOBS with MAB) shows a dynamic range of SMNOBS at least 0-500 nM with a slope of 1.3×10^{-4} nM^{-1} and R^2 of 0.99.

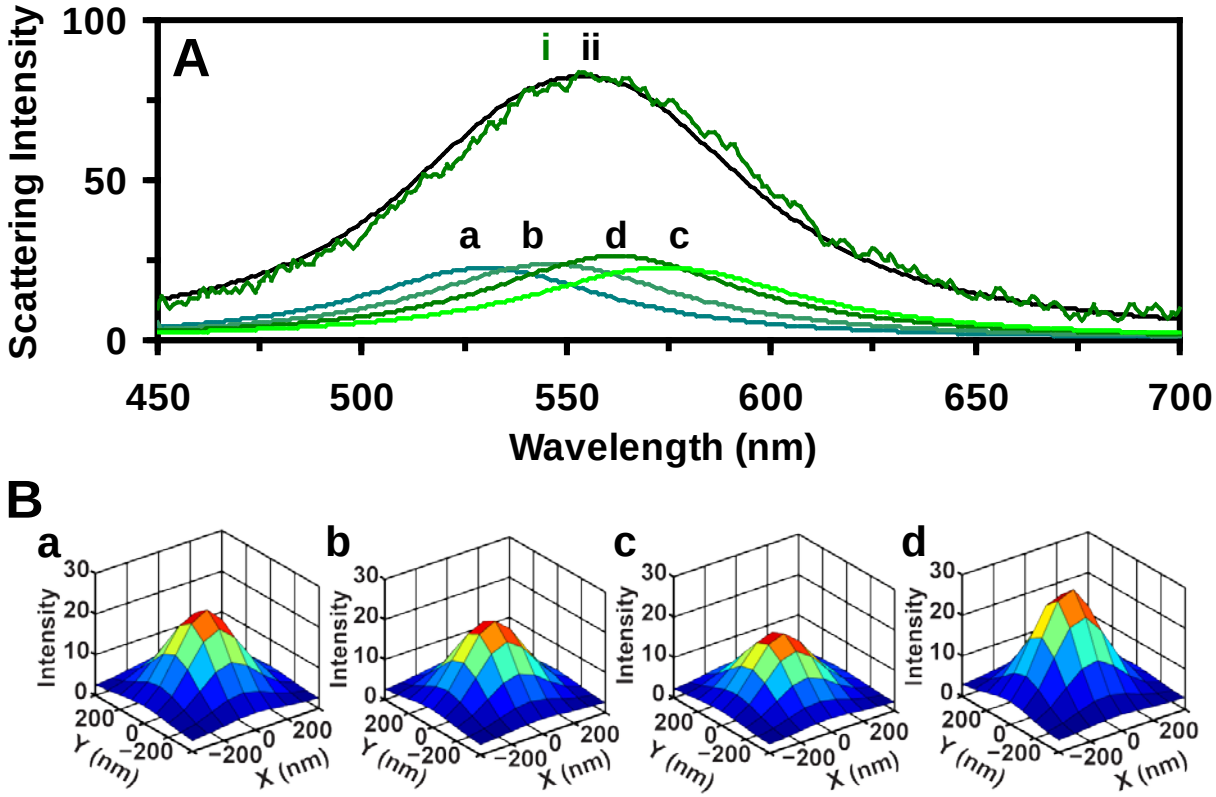

Fig. S4: Real-time mapping of number and centroids of individual L-R complexes (bound SMNOBS) located in spot-(a) (a cluster of single L-R complexes located within optical diffraction limit) on single live cells using deconvolution and PSF. **(A)**: (i) LSPR spectrum of the cluster in spot-(a) as circled in Fig 4C; (a-d) deconvoluted LSPR spectra of individual L-R complexes; and (ii) sum of deconvoluted LSPR spectra of (a-d), show λ_{max} (FWHM): (i) 553 (88); (ii) 554 (88); (a) 530 (68); (b) 546 (75); (c) 574 (81); (d) 562 (71) nm. **(B)** Plots of scattering intensity of each individual complex with each deconvoluted LSPR spectrum of (a-d) in (A) versus its location, respectively. As determined by PSF, the precise location (centroid) of each individual complex in (a-d) is (38.5, 60.8), (34.0, 44.0), (43.3, 51.4), (54.3, 50.5) nm, respectively.

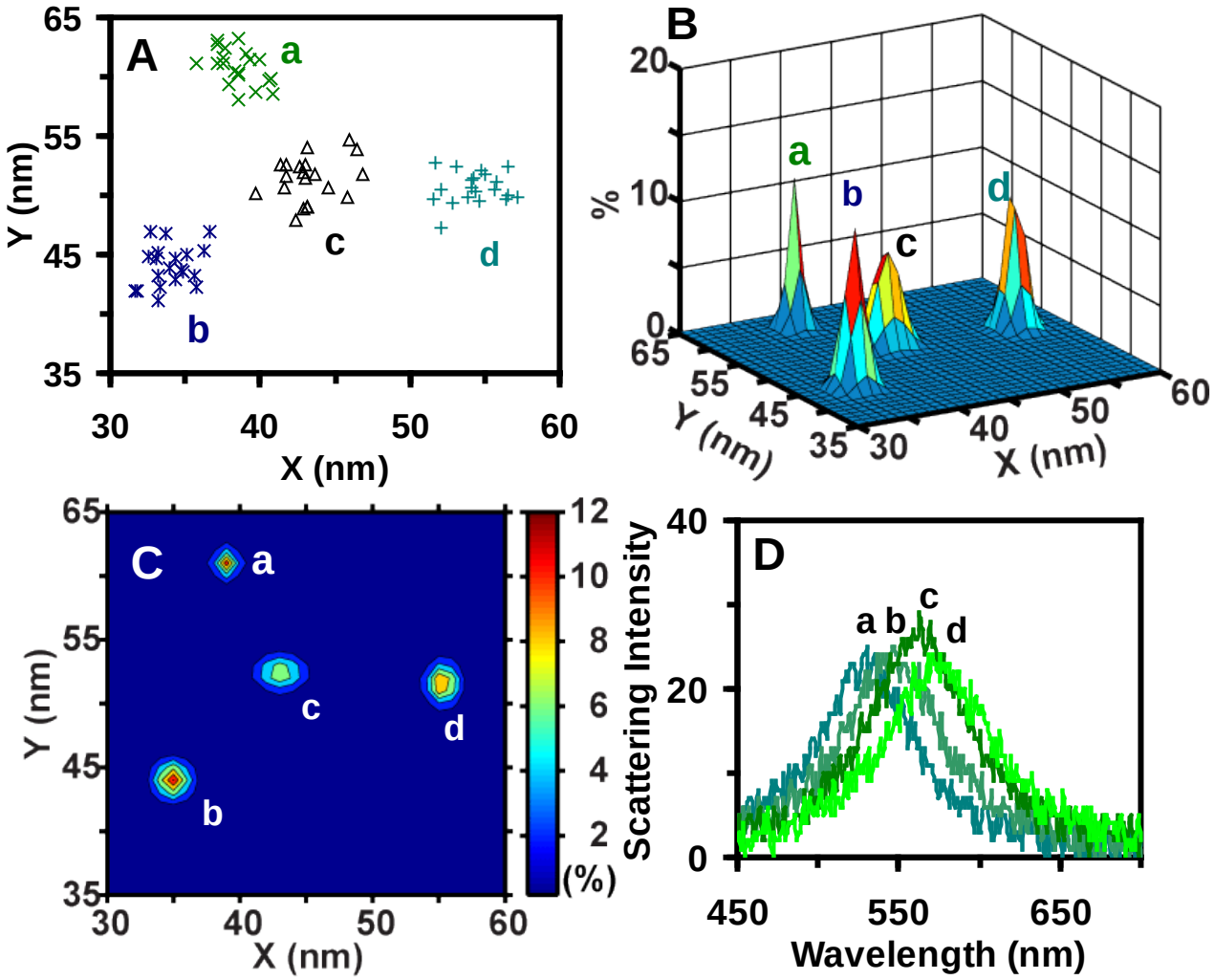

Fig. S5: Nanometer-resolution imaging of individual L-R complexes (bound SMNOBS) located within optical diffraction limit, spot-(a) in Fig. 4C, on single live cells using PHOTON. **(A)** Plots of distributions of precise locations (centroids) of single L-R complexes determined by PSF. Twenty repeated measurements of Fig S4 are made for each complex and each point represents one measurement. **(B)** 2D Gaussian fitting of the distributions of 20 precise locations of each complex in (A). **(C)** The contour plots of (B) show centroids of single complexes in (a-d): (38.5±1.4, 60.8±1.5), (54.3±1.7, 50.6±1.3), (43.3±1.8, 51.4±1.9), and (40.0±1.4, 44.0±1.7) nm, respectively. **(D)** LSPR spectra of single complexes at the locations in (C) show λ_{max} (FWHM): (a) 530 (63); (b) 547 (69); (c) 573 (76) and (d) 564 (77) nm.

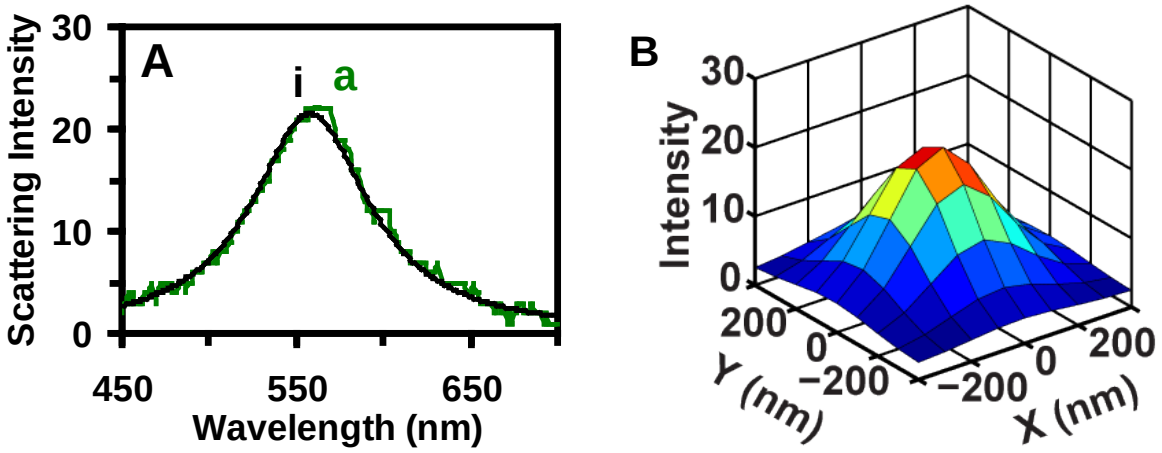

Fig. S6: Mapping of the number and centroid of single L-R complex (bound SMNOBS) located within optical diffraction limit, spot-(b), on single live cells, using deconvolution and PSF. **(A)**: (i) LSPR spectrum of the cluster of single L-R complexes in spot-(b) circled in Fig 4D; (a) deconvoluted LSPR spectrum of the complex shows λ_{max} (FWHM) at: (i) 562 (75) and (a) 558 (75) nm. **(B)** Plot of scattering intensity of the complex with deconvoluted LSPR spectrum in (A) versus its locations. The precise location (centroid) of the complex in (B) is (53.0, 47.0) nm, as determined by PSF.

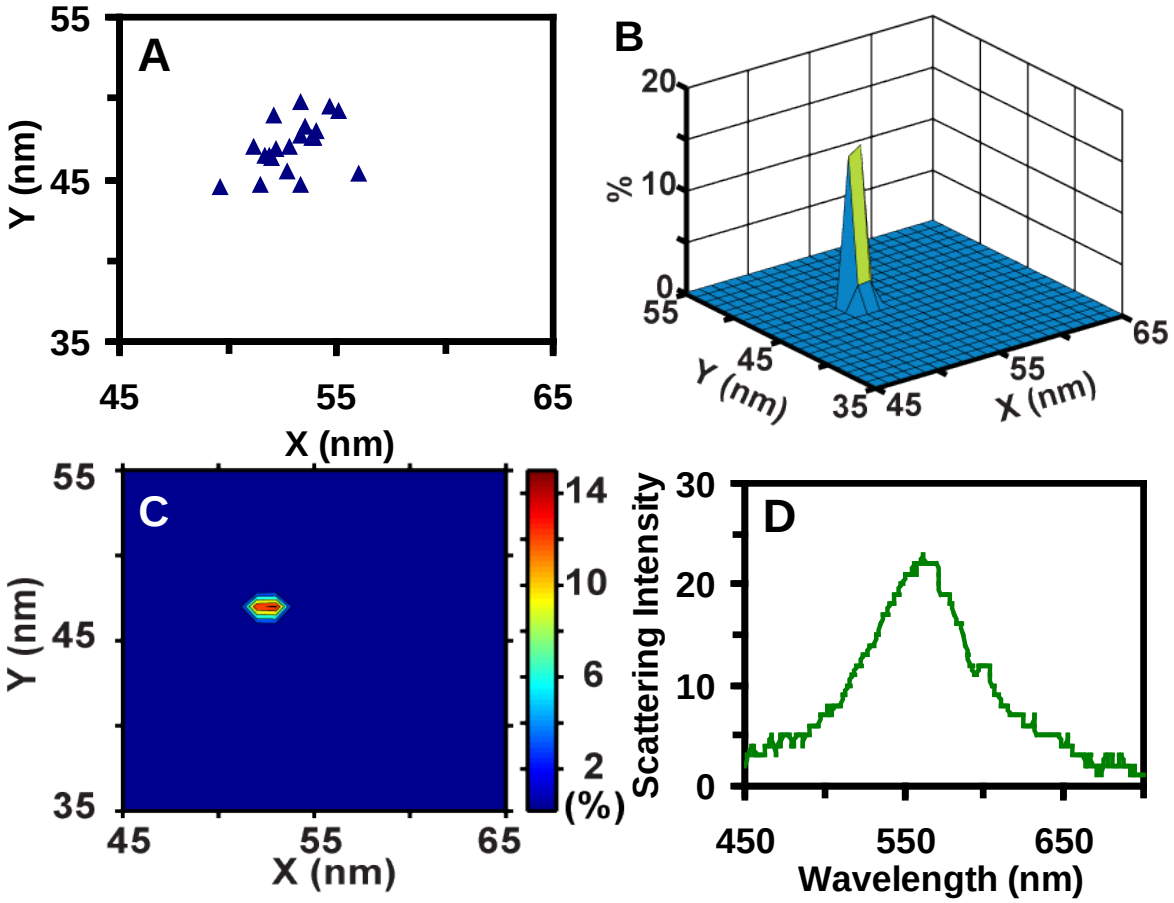

Fig. S7: Nanometer-resolution imaging of single L-R complexes (bound SMNOBS) located within optical diffraction limit, spot-(b) in Fig 4D, on single live cells, using PHOTON. **(A)** Plot of distribution of centroids of the complex determined by PSF. Twenty repeated measurements of Fig S6 are made, and each point represents one measurement. **(B)** 2D Gaussian fitting of the distribution of 20 precise locations of the complex in (A). **(C)** The contour plot of (B) shows that centroid of the complex locates at (53.0±1.5, 47.0±1.6) nm. **(D)** LSPR spectrum of the complex at the location in (C) shows λ_{max} (FWHM) at 562 (75) nm.

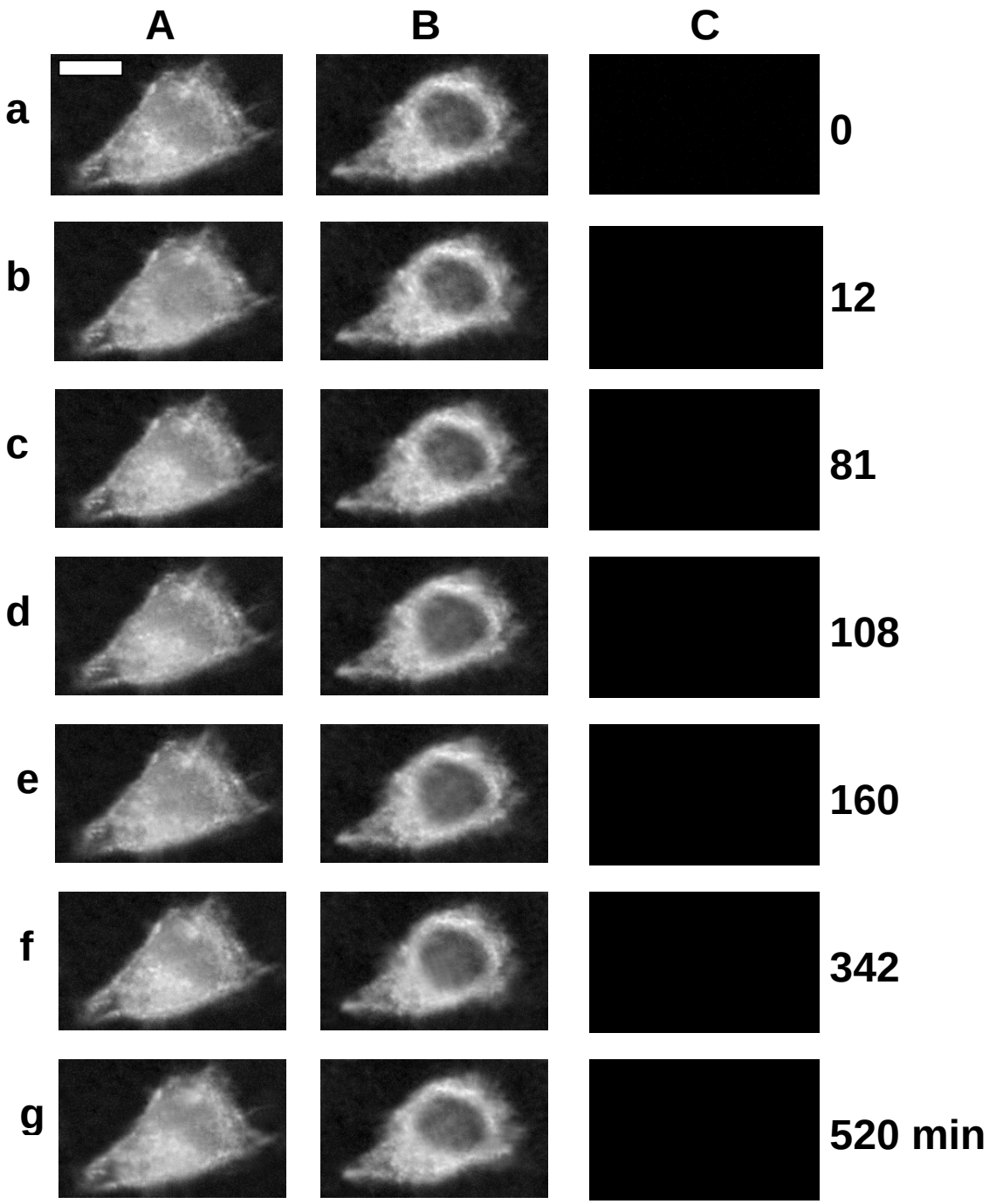

Fig. S8: Real-time imaging of single live cells incubated with the cell culture medium over time (control experiment of Fig. 6). Snap shots of sequential optical images: **(A)** on the plasma membrane and **(B)** in the cytoplasm of a live cell, and **(C)** magic-red fluorescent images of (B), at (a) 0, (b) 12, (c) 81, (d) 108, (e) 160, (f) 342, and (g) 520 min. Around 10 individual cells are imaged simultaneously over 900 min for each measurement, and 26 individual cells are studied for three measurements. The temporal resolution is 100 ms and observation resolution is 25 s. Scale bar is 10 μm for all images.

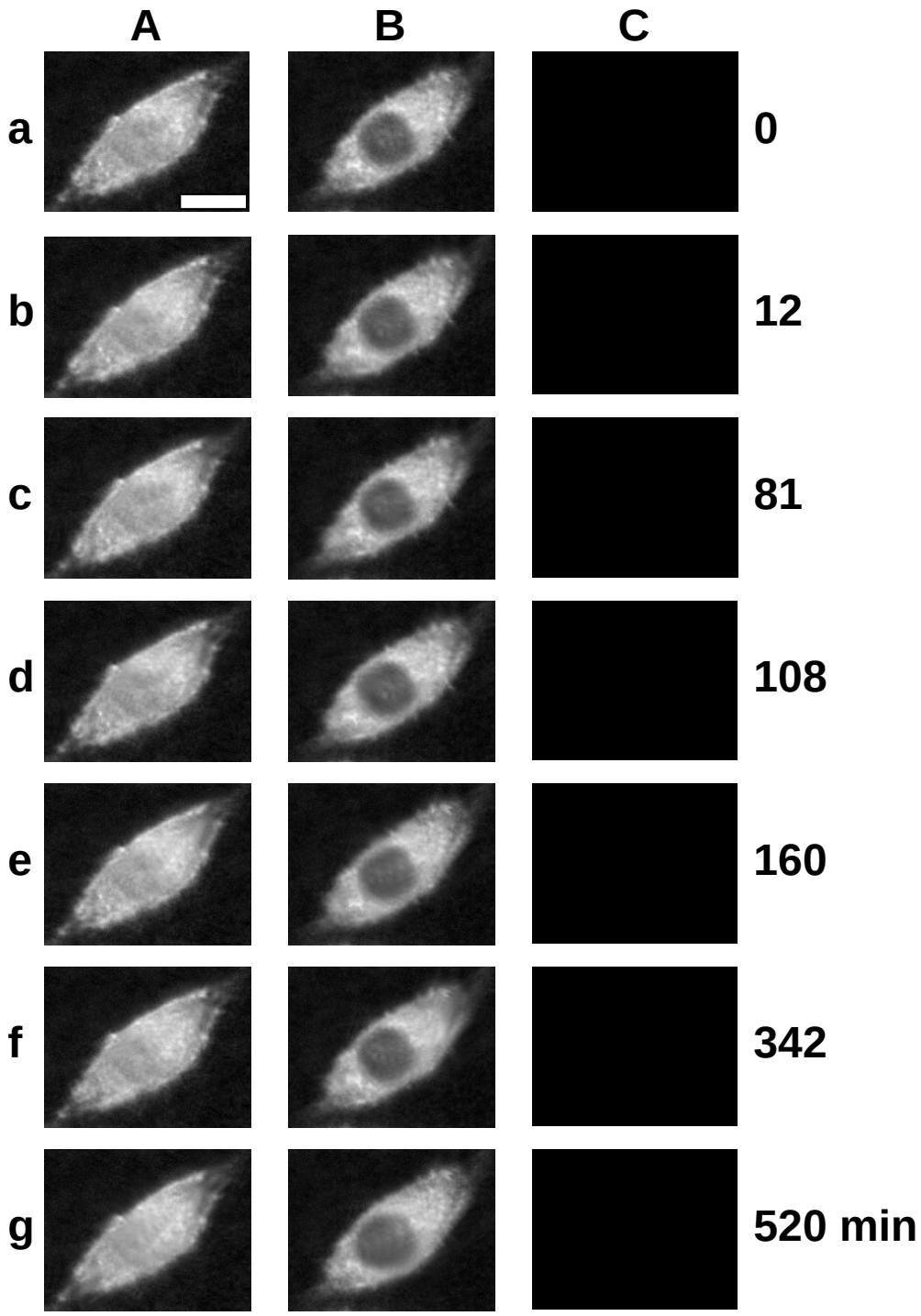

Fig. S9: Real-time imaging of single live cells incubated with AgMMUA (4.6 nM) in the medium over time (control experiment of Fig. 6). Snap shots of sequential optical images: **(A)** on the plasma membrane and **(B)** in the cytoplasm of a live cell, and **(C)** magic-red fluorescent images of (B), at (a) 0, (b) 12, (c) 81, (d) 108, (e) 160, (f) 342, and (g) 520 min. About 10 individual cells are imaged over 900 min simultaneously for each measurement, and 26 individual cells are studied for three measurements. The temporal resolution is 100 ms and observation resolution is 25 s. Scale bar is 10 μm for all images.